JOC*Article*

Theoretical Study of the Orientation Rules in Photonucleophilic Aromatic Substitutions

B. Pintér,[†,‡] F. De Proft,*[,‡] T. Veszprémi,[†] and P. Geerlings[‡]

Inorganic and Analytical Chemistry Department, Budapest University of Technology and Economics (BUTE), Szent Gellért tér 4, 1521 Budapest, Hungary, and Eenheid Algemene Chemie (ALGC), Faculteit Wetenschappen, Vrije Universiteit Brussel (VUB), Pleinlaan 2, 1050 Brussels, Belgium

fdeprof@vub.ac.be

Received July 10, 2007

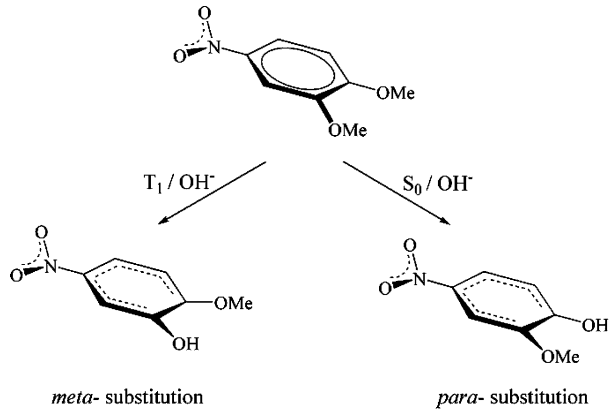

The photonucleophilic aromatic substitution reactions of nitrobenzene derivatives were studied by ab initio and Density Functional Theory methods. The photohydrolysis is shown to proceed via an addition−elimination mechanism with two intermediates, except in the case of a chlorine leaving group. Depending on the substituents, the addition step, the elimination step, or the radiationless transition is the rate-determining process. The solvent effect on the S_N2 Ar* reactions was evaluated by a continuum model. Next, the regioselectivity of the addition step is investigated within the framework of the so-called spin-polarized conceptual density functional theory. It is shown that the preference observed for the meta or para (with respect to the NO_2 group) pathways in the addition step can be predicted by using the spin-polarized Fukui functions applied for the prereactive π-complex.

1. Introduction

The absorption of a photon in the ultraviolet or visible regions of the electromagnetic spectrum results in an electronic excitation of a molecule that then can undergo reactions that are either unfavorable or forbidden in the ground state system. One of the most fascinating photochemical processes is the photonucleophilic aromatic substitution, discovered in 1956.[1] The unique feature of these reactions is the inversion of the orientation rules when going from the ground state to the excited state nucleophilic substitution. In excited states, electron-withdrawing groups orient the incoming nucleophile to the meta position, whereas thermally, these groups are ortho and para directing. Also, strong electron-releasing substituents may activate the ring for a nucleophilic attack and direct the approaching nucleophile to ortho or para positions.[2] Three major mechanisms are relevant for reaction after the initial light absorption:[3] (a) after electron transfer to the aromatic substrate a negatively charged ligand is eliminated from the excited anion and the nucleophilic reagents attack on the radical compound formed, (b) electron transfer occurs from the excited molecule to an electron acceptor and the resulting radical cation rapidly reacts with the nucleophile, or (c) the reaction goes by an addition−elimination mechanism through a σ-complex intermediate.

* Author to whom correspondence should be sent.
† Budapest University of Technology and Economics.
‡ Vrije Universiteit Brussel.

(1) Havinga, E.; de Jongh, R. O.; Dorst, W. *Recl. Trav. Chim. Pays-Bas* **1956**, *75*, 378.

(2) Turro, N. J. *Modern molecular photochemistry*; Benjamin/Cummings: Menlo Park, CA, 1978; p 404.

(3) Van Riel, H. C. H. A; Lodder, G.; Havinga, E. *J. Am. Chem. Soc.* **1981**, *103*, 7257.

10.1021/jo701392m CCC: $40.75
Published on Web 01/24/2008

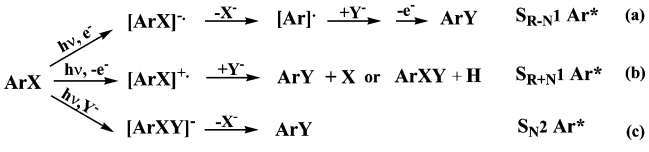

The $S_{R-N}1$ Ar* mechanism is a six-step radical chain process that was invoked early on to explain the reactivity of monosubstituted benzene derivatives with an enolate ion under irradiation.[4] In addition, several photoaminations were found to take place through this mechanism and amines of low ionization potential were found to be required in order to start the reaction.[5] In the reactions where the excited aromatic compound is involved as electron donor ($S_{R+N}1$ Ar*), the radical cation formed can be stabilized by electron-donating substituents, which direct the incoming nucleophile to the para (and ortho) position.[1,3] In this case, the decisive step is the electron transfer from the photoexcited arene to the electron acceptor.[3]

The first step of the S_N2 Ar* mechanism was proposed to be the formation of a σ-complex via the attack of the nucleophile on the excited aromatic system. Time-resolved electronic absorption spectroscopy measurements provided evidence for this mechanism; van Eijk et al. detected the σ-complex intermediate.[6] Next, one of the competing nucleophiles leaves the system and the aromatic π system recovers. The reactions of the following substituted nitrobenzenes were proposed to follow the S_N2 Ar* mechanism.[7] Reaction of 3-methoxynitrobenzene (*m*-nitroanisole, ***m*NA**, see Scheme 1 for numbering) with hydroxide ions gives *m*-nitrophenol in an efficient and regioselective manner[7,8] whereas photohydrolysis of 2-methoxynitrobenzene (*o*-nitroanisole, ***o*NA**) provides the mixture of *o*-nitrophenol and *o*-methoxyphenol (31:3).[7] Letsinger et al. demonstrated that the substitution of the nitro group is also an effective competing reaction with the formation of *p*-nitrophenol in the analogous reaction of *p*-nitroanisole (***p*NA**).[9] Also, the formation of 2-methoxy-5-nitrophenol was observed under the irradiation of 3,4-dimethoxynitobenzene (4-nitroveratrole) in water containing 2% tetrahydrofuran.[10] In contrast the thermal hydrolysis of 4-nitroveratrole gives the para rather than the meta product[11] (Scheme 2).

The overwhelming preference for meta substitution in the S_N2 Ar* mechanism reactions is a consequence of the strong electron-withdrawing effect of the nitro group;[12] in addition this effect is intensified by the methoxy substituent in 4-nitroveratrole being an electron-releasing group.[7]

There is still some debate on the orientation effect of the NO_2 group in nucleophilic substitutions of excited state arenes.

SCHEME 1

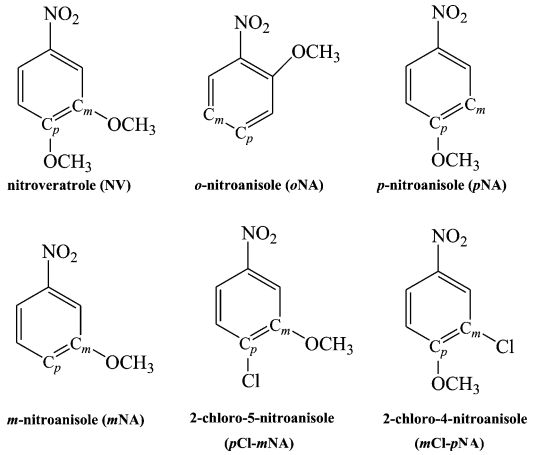

SCHEME 2

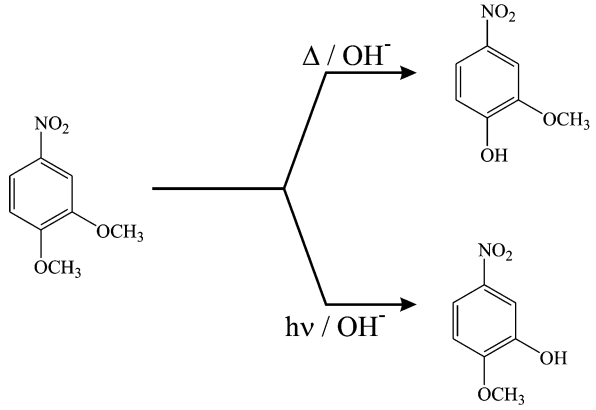

The charge distribution was found to be a particularly effective predictor of regioselectivity suggesting a charge-controlled process.[7] Other authors advocated the S_N2 Ar* process to be HOMO controlled.[13] Combining these results leads to the hypothesis that the orientation-determining step is the addition of the nucleophile to the excited aromatic compound. Cantos and co-workers, however, stated that the stability of the σ-complex intermediate controls the regioselectivity of the reaction.[14] In other cases the energy gaps between the singlet and triplet σ-complexes were referred to as the determining factor.[3]

Photoamination[14,15] and photocyanation[13a] provide a wider variety of photonucleophilic aromatic substitutions than photohydrolysis. The mechanism of the former process is determined by the nucleophile (primary, secondary amine, etc.), the substituents on the aromatic ring, the electronic state of the reactant, and the solvent.[16] The operative mechanisms for photocyanations are S_N2 Ar* and $S_{R+N}1$ Ar*, whereas photo-

(4) (a) Rossi, R. A.; Bunnett, J. F. *J. Org. Chem.* **1973**, *38*, 1407. (b) Bunnett, J. F. *Acc. Chem. Res.* **1978**, *11*, 413.

(5) (a) Bunce, N. J.; Cater, S. R.; Scaiano, J. C.; Johnston, L. J. *J. Org. Chem.* **1987**, *52*, 4214. (b) Cervelló, J.; Figueredo, M.; Marquet, J.; Moreno-Manas, M.; Bertrán, J.; Lluch, J. M. *Tetrahedron Lett.* **1984**, *25*, 4147.

(6) van Eijk, A. M. J.; Huizer, A. H.; Varma, C. A. G. O.; Marquet, J. *J. Am. Chem. Soc.* **1989**, *111*, 88.

(7) Cornelisse, J.; Havinga, E. *Chem. Rev.* **1975**, *75*, 353.

(8) (a) Havinga, E. *K. Ned. Akad. Wet., Versl. Gewone Vergad. Afd. Natuurk.* **1961**, *70*, 52. (b) Havinga, E.; de Jongh, R. O. *Bull. Soc. Chim. Belg.* **1962**, *71*, 803.

(9) Letsinger, R. L.; Ramsay, O. B.; McCain, J. H. *J. Am. Chem. Soc.* **1965**, *87*, 2945.

(10) (a) Havinga, E.; Cornelisse, J. *Pure Appl. Chem.* **1976**, *47*, 1. (b) van Vliet, A. Thesis, Leiden, 1969. (c) Cornelisse, J.; de Grinst, G. P.; Havinga, E. *Adv. Phys. Org. Chem.* **1976**, *11*, 225.

(11) Letsinger, R. T.; Colb, A. *J. Am. Chem. Soc.* **1975**, *94*, 3665.

(12) Reference 2, p 405.

(13) (a) Konstantinov, A. D.; Bunce, N. J. *J. Photochem. Photobiol. A*: *Chem.* **1999**, *125*, 63. (b) Mutai, K.; Yokoyama, K.; Kanno, S.; Kobayashi, K. *Bull. Chem. Soc. Jpn.* **1982**, *55*, 1112.

(14) Cantos, A.; Marquet, J.; Moreno-Manas, M.; González-Lafont, A.; Lluch, J. M.; Bertrán, J. *J. Org. Chem.* **1990**, *55*, 3303.

(15) (a) Cantos, A.; Marquet, J.; Moreno-Manas, M. *Tetrahedron Lett.* **1987**, *28*, 4191. (b) Cantos. A.; Marauet. J.: Moreno-Manas, M.: Castelló, A. *Tetrahedron* **1988**, *44*, 2607. (c) Van Eijk, A. M. J.; Huizer, A. H.; Varma, C. A. G. O.; Marquet, J. *J. Am. Chem. Soc.* **1989**, *111*, 88. (d) Manickam, M. C. D.; Pitchumani, K.; Srinivasan, C. *J. Chem. Sci.* **2003**, *115*, 273.

(16) Zanini, G. P.; Montejano, H. A.; Cosa, J. J.; Previtali, C. M. J. *Photochem. Photobiol. A*: *Chem.* **1997**, *107*, 9.

aminations mainly occur via S_N2 Ar* (for high ionization potential amines) and $S_{R-N}1$ Ar* (for low ionization potential amines).

The purpose of this article is twofold: (1) to introduce a reliable but simple method for obtaining the reactive positions to predict the regioselectivity of excited aromatic compounds and (2) to investigate in detail the mechanism of the S_N2 Ar* process including the characterization of the intermediates and determination of the rate-decisive steps using ab initio and density functional calculations. The former investigation is a sequel to our earlier initial papers on the use of DFT descriptors in orientation and site selectivity problem in various types of organic reactions.[17]

2. Theory and Computational Details

Next to its well-established computational advantages, density functional theory (DFT) proved to be a source for introducing and/or precising a series of chemical concepts and principles (such as Pearson's Hard and Soft Acids and Bases Principle[18]) readily used by chemists but often defined on an empirical basis. Now a series of global and local quantities, the so-called reactivity descriptors or indices, founded within the "conceptual DFT"[19] are available to the practicing chemists to describe the extent of the response of a molecular system toward perturbations in either its number of electrons, N, its external (i.e., due to the nuclei) potential, $v(\underline{r})$, or both.[19] The Fukui function introduced by Parr and Yang[20] represents the response of the system's electron density $\rho(\underline{r})$ due to a perturbation in its total number of electrons N at a constant external potential $v(\underline{r})$.

$$f(\underline{r}) = (\partial\rho(\underline{r})/\partial N)_{v(\underline{r})} \tag{1}$$

Within the framework of spin-polarized DFT,[21] besides N and $v(\underline{r})$, the spin number N_S, being the difference between N_α and N_β, is introduced as the basic variable for four types of Fukui functions and they can be written as[22,23]

$$f_{NN}(\underline{r}) \equiv \left[\frac{\partial\rho(\underline{r})}{\partial N}\right]_{N_S,v(\underline{r})} \tag{2}$$

$$f_{SN}(\underline{r}) \equiv \left[\frac{\partial\rho_S(\underline{r})}{\partial N}\right]_{N_S,v(\underline{r})} \tag{3}$$

$$f_{NS}(\underline{r}) \equiv \left[\frac{\partial\rho(\underline{r})}{\partial N_S}\right]_{N,v(\underline{r})} \tag{4}$$

$$f_{SS}(\underline{r}) \equiv \left[\frac{\partial\rho_S(\underline{r})}{\partial N_S}\right]_{N,v(\underline{r})} \tag{5}$$

These derivatives are evaluated at constant external potential and, in our case, at constant external magnetic field equal to zero. $\rho(\underline{r}) = \rho_\alpha(\underline{r}) + \rho_\beta(\underline{r})$ and $\rho_S(\underline{r}) = \rho_\alpha(\underline{r}) - \rho_\beta(\underline{r})$ are the electron and spin densities, respectively. In the present application, one of the reaction partners, the arene, is in its excited triplet state for which the electron densities of the α and β electrons are different, corresponding to a spin-polarized chemical system.

Within a frozen orbital approximation, the spin-polarized Fukui functions for nucleophilic attack can be computed by using the HOMO and LUMO shape factors, proposed by Galvan et al.:[23]

$$f^+_{NN,k} = \frac{1}{2}[\sigma_k^{LUMO,\alpha} + \sigma_k^{LUMO,\beta}] \tag{6}$$

To calculate the shape factors via molecular spin orbital approximation, an atomic basis-set partitioning has been used:[24]

$$\sigma_k^{LUMO,\alpha} = \frac{1}{n_{deg,LUMO,\alpha}} \sum_{g_{LUMO,\alpha}}^{n_{deg,LUMO,\alpha}} \sum_{\mu\in k} \sum_{\nu} c_{\mu,g_{LUMO,\alpha}} c_{\nu,g_{LUMO,\alpha}} S_{\mu\nu} \tag{7}$$

$$\sigma_k^{LUMO,\beta} = \frac{1}{n_{deg,LUMO,\beta}} \sum_{g_{LUMO,\beta}}^{n_{deg,LUMO,\beta}} \sum_{\mu\in k} \sum_{\nu} c_{\mu,g_{LUMO,\beta}} c_{\nu,g_{LUMO,\beta}} S_{\mu\nu} \tag{8}$$

where σ_k represents the shape factors of corresponding molecular orbital, $c_{\mu,g}$ are the molecular orbital coefficients, and $n_{deg,mo}$ is the number of degenerate frontier orbitals of the given specified spin state (i.e., a crude average for possible effects due to the presence of degenerate molecular frontier spin orbitals).

The geometrical structures corresponding to stationary points (local minima, saddle points) along the reaction path for a series of S_N2 Ar* rearrangements have been determined by DFT calculations using the B3LYP[25] functional and second-order Møller−Plesset perturbation theory[26] (MP2). All calculations were performed with the Gaussian03[27] software package. The spin unrestricted (U)-B3LYP/6-311+G(d)[28] and (U)MP2/6-31+G(d) levels are employed since the reactions involve triplet species. For the latter level of theory, it was confirmed that spin contamination is in the range of 10% of the exact expectation value of $\langle S^2\rangle$ for the triplet state, except for the case of mTS1mClpNA(t), where it is only slightly higher (2.2223). At the B3LYP level, stationary points were characterized by harmonic frequency analysis as local minima or first-order saddle points. The calculations for the product-leaving group π-complexes ***m*C2[*p*Cl-*m*NA](t)**, ***m*C2[*m*NA](t)**, and ***p*C2[*m*Cl-*p*NA](t)** yield one imaginary frequency with very small absolute values (8.6i, 16.7i, and 18.3i cm^{-1}, respectively). In the π-complexes ***p*C2[*p*NA]-(t)** and ***p*C2[NV](s)** there is an imaginary frequency corresponding

(17) (a) Tielemans, M.; Areschka, V.; Colomer, J.; Promel, R.; Langenaeker, W.; Geerlings, P. *Tetrahedron* **1992**, *48*, 10575. (b) Damoun, S.; Van de Woude, G.; Mendez, F.; Geerlings, P. *J. Phys. Chem. A* **1997**, *101*, 886. (c) Langenaeker, W.; De Proft, F.; Geerlings, P. *J. Phys. Chem. A* **1998**, *102*, 5944. (d) Nguyen, L. T.; Le, T. N.; De Proft, F.; Chandra, A. K.; Langenaeker, W.; Nguyen, M. T.; Geerlings, P. *J. Am. Chem. Soc.* **1999**, *121*, 5992. (e) Geerlings, P.; De Proft, F. *Int. J. Quantum Chem.* **2000**, *80*, 227. (f) De Proft, F.; Fias, S.; Van Alsenoy, C.; Geerlings, P. *J. Phys. Chem. A* **2005**, *109*, 6335.

(18) (a) Pearson, R. G. *J. Am. Chem. Soc*. **1963**, *85*, 3533. (b) Pearson, R. G. *Science* **1966**, *151*, 172. (c) Chattaraj, P. K.; Lee, H.; Parr, R. G. *J. Am. Chem. Soc*. **1991**, *113*, 1855. (c) Ayers, P. W. *J. Chem. Phys*. **2005**, *122*, 141102. (d) Chattaraj, P. K.; Ayers, P. W. *J. Chem. Phys*. **2005**, *123*, 086101. (e) Ayers, P. W.; Parr, R. G.; Pearson, R. G. *J. Chem. Phys*. **2006**, *124*, 194107.

(19) (a) Parr, R. G.; Yang, W. *Density Functional Theory of Atoms and Molecules*; Oxford University Press: New York, 1989. (b) Parr, R. G.; Yang, W. *Annu. Rev. Phys. Chem.* **1995**, *46*, 701. (c) Kohn, W.; Becke, A. D.; Parr, R. G. *J. Phys. Chem.* **1996**, *100*, 12974. (d) Chermette, H. *J. Comput. Chem.* **1999**, *20*, 129. (e) Geerlings, P.; De Proft, F.; Langenaeker, W. *Adv. Quantum Chem.* **1999**, *33*, 303. (f) Geerlings, P.; De Proft, F.; Langenaeker, W. *Chem. Rev.* **2003**, *103*, 1793.

(20) Parr, R. G.; Yang, W. *J. Am. Chem. Soc.* **1984**, *106*, 4049.

(21) (a) Von Bart, U.; Hedin, L. *J. Phys. C* **1972**, *5*, 1629. (b) Rajagopal, A. K.; Callaway, J. *Phys. Rev. B* **1973**, *7*, 1912. (c) Gunnarson, O.; Lundqvist, B. I. *Phys. Rev. B* **1976**, *13*, 4274.

(22) Chamorro, E.; Santos, J. C.; Escobar, C. A.; Perez, P. *Chem. Phys. Lett.* **2006**, *431*, 210.

(23) Galván, M.; Vela, A.; Gázquez, J. L. *J. Phys. Chem.* **1988**, *92*, 6470.

(24) Contreras, R. R.; Fuentealba, P.; Galvan, M.; Perez, P. *Chem. Phys. Lett.* **1999**, *304*, 405.

(25) (a) Becke, A. D. *J. Chem. Phys.* **1993**, *98*, 5648. (b) Lee, C.; Yang, W.; Parr, R. G. *Phys. Rev. B* **1988**, *37*, 785. (c) Stephens, P. J.; Devlin, F. J.; Chabalowski, C. F.; Frisch, M. J. *J. Phys. Chem.* **1994**, *98*, 11623.

(26) (a) Møller, C.; Plesset, M. S. *Phys. Rev.* **1934**, *46*, 618. (b) Head-Gordon, M.; Pople, J. A.; Frisch, M. J. *Chem. Phys. Lett.* **1988**, *153*, 503. (c) Frisch, M. J.; Head-Gordon, M.; Pople, J. A. *Chem. Phys. Lett.* **1990**, *166*, 275. (d) Frisch, M. J.; Head-Gordon, M.; Pople, J. A. *Chem. Phys. Lett.* **1990**, *166*, 281.

to the rotation of the methyl group around the C−O bond of the methoxy group and bond formation between the oxygen atom of the methoxy and hydrogen atom of the OH group, respectively. As a result, these π-complexes could not be optimized accurately as their geometries correspond to first-order saddle points and their relative energies are not considered.

It was found that the DFT approach provides a good description of the triplet potential energy surfaces and predicts lower barriers for meta than para attack, which is in good agreement with the experimental evidence. On the other hand, the (U)MP2/6-31+G(d) method gives the reverse result in several cases (**NV(t)**, ***m*NA(t)**, ***p*Cl-*m*NA(t)**, and ***m*Cl-*p*NA(t)**). To test its accuracy, CCSD(T)/6-31+G(d)//(U)MP2/6-31+G(d) energies were calculated for the first transition state (addition step) of both para and meta reaction path of the reference **NV(t)** system; these calculations revealed a lower barrier for meta with respect to para in agreement with the DFT barrier ordering.[29] The solvent effect was investigated by using polarizable continuum model calculations at the PCM/UB3LYP/6-31+G(d)[30] level. The calculations were carried out for the reference nitroveratrole in triplet state **NV(t)**, using the relative dielectric constant of water.

Charges based on electrostatic potential (ChelpG) introduced by Breneman and Wiberg[31] were obtained on all arene reactants at the (U)B3LYP/6-311+G(d) and (U)B3LYP/6-311G(d) levels. The condensed spin-polarized Fukui functions $f^{+}_{NN,C}$ for the π-complexes were computed on the various ring carbon atoms at the (U)B3LYP/6-311G(d) level using approximation (6); to calculate the $S_{\mu\nu}$ values simple modifications to the 1601.F routine of Gaussian have been introduced.[24]

3. Results and Discussion

As Carey and Sundberg wrote: "Identification of the intermediates in a multistep reaction is a major objective of studies of reaction mechanisms. When the nature of each intermediate is fairly well understood, a great deal is known about the reaction mechanism."[32] Accordingly, the first part of this paper will deal with the mechanism of the photonucleophilic aromatic substitution and with the different species involved in the reaction. In this paper, we have investigated in detail the photohydrolysis of the compounds given in Scheme 1. The reaction of nitroveratrole (**NV**) was studied because it is one of the cleanest photoreactions known to occur in the triplet state. It was chosen as the reference reaction in this paper and we will discuss both its photochemical (triplet) and thermal (singlet) hydrolysis in more detail. In addition, three nitroanisole derivatives (***o*NA**, ***p*NA**, ***m*NA**) have been considered since their photonucleophilic aromatic substitutions were studied extensively in the past.

SCHEME 3

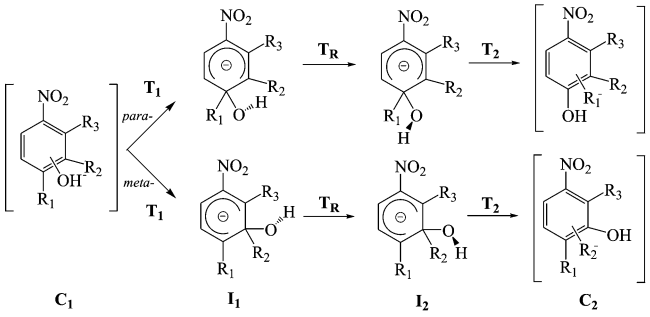

We have not investigated the details concerning the photoprocess leading to the formation of T_1 after initial photoexcitation from S_0 to an excited singlet state. However, we note that nitrobenzene derivatives are known to relax from S_1 to T_1 by a very efficient intersystem crossing (ISC) caused by direct spin−orbit coupling between S_1 and T_2 states.[33]

In most cases we found that the triplet meta and para reaction paths are multistep processes proceeding through three transition states and two σ-complex intermediates (Scheme 3). As an illustration, molecular models along the para pathway in the case of **NV(t)** are given in Figure 1. Initially, the approaching nucleophile interacts with the triplet π-system and the two reactants form a weak π-complex. The first and the last transition state correspond to the addition and the elimination steps of reaction, respectively. In the intermediate region two σ-complexes were found which easily convert to each other via the rotation of the OH group around the C−O bond. In both intermediates the π-system is broken. A second π-complex is formed from the product and the leaving group in the last step. This proposed reaction profile has been supported by IRC calculations.

(a) The Hydrolysis of Nitroveratrole. The hydrolysis induced by heating (thermal) and the one induced by light (photochemical) were investigated by modeling the reactions in the lowest singlet and in triplet states (Figure 2). Table 1 contains the relative energies and Gibbs free energies, compare to **C1** (see Figure 1 and Scheme 1 for clarification) of the molecular species involved in these reactions. Figure 2 shows schematic Gibbs free energy profiles for the para and meta pathways of nitroveratrole found on the S_0 and T_1 states potential energy surfaces (PES). Both the photochemical and the thermal nucleophilic aromatic substitution of **NV** are predicted to occur via a three-step mechanism described above. The different outcome of the excited and ground state reactions finds a simple rationalization in energy profiles,[34] which show that the barrier

(27) Frisch, M. J.; Trucks, G. W.; Schlegel, H. B.; Scuseria, G. E.; Robb, M. A.; Cheeseman, J. R.; Montgomery, J. A., Jr.; Vreven, T.; Kudin, K. N.; Burant, J. C.; Millam, J. M.; Iyengar, S. S.; Tomasi, J.; Barone, V.; Mennucci, B.; Cossi, M.; Scalmani, G.; Rega, N.; Petersson, G. A.; Nakatsuji, H.; Hada, M.; Ehara, M.; Toyota, K.; Fukuda, R.; Hasegawa, J.; Ishida, M.; Nakajima, T.; Honda, Y.; Kitao, O.; Nakai, H.; Klene, M.; Li, X.; Knox, J. E.; Hratchian, H. P.; Cross, J. B.; Bakken, V.; Adamo, C.; Jaramillo, J.; Gomperts, R.; Stratmann, R. E.; Yazyev, O.; Austin, A. J.; Cammi, R.; Pomelli, C.; Ochterski, J. W.; Ayala, P. Y.; Morokuma, K.; Voth, G. A.; Salvador, P.; Dannenberg, J. J.; Zakrzewski, V. G.; Dapprich, S.; Daniels, A. D.; Strain, M. C.; Farkas, O.; Malick, D. K.; Rabuck, A. D.; Raghavachari, K.; Foresman, J. B.; Ortiz, J. V.; Cui, Q.; Baboul, A. G.; Clifford, S.; Cioslowski, J.; Stefanov, B. B.; Liu, G.; Liashenko, A.; Piskorz, P.; Komaromi, I.; Martin, R. L.; Fox, D. J.; Keith, T.; Al-Laham, M. A.; Peng, C. Y.; Nanayakkara, A.; Challacombe, M.; Gill, P. M. W.; Johnson, B.; Chen, W.; Wong, M. W.; Gonzalez, C.; Pople, J. A. *Gaussian 03*, Revision C.02; Gaussian, Inc.: Wallingford, CT, 2004.

(28) For a detailed account on these types of basis sets, see: Hehre, W. J.; Radom, L.; Schleyer, P. v. R.; Pople, J. A. *Ab Initio Molecular Orbital Theory*; Wiley: New York, 1986.

(29) The total electronic energies for ***m*T1[NV](t)** and ***p*T1[NV](t)** at the CCSD(T)/6-31+G(d)//(U)MP2/6-31+G(d) level are −739.496610 and −739.467558 au, respectively.

(30) (a) Miertus, S.; Scrocco, E.; Tomasi, J. *Chem. Phys.* **1981**, *55*, 117. (b) Cossi, M.; Rega, N.; Scalmani, G.; Barone, V. *J. Chem. Phys.* **2001**, *114*, 5691. (c) Cammi, R.; Mennucci, B.; Tomasi, J. *J. Phys. Chem. A* **1999**, *103*, 9100.

(31) Breneman, C. M.; Wiberg, K. B. *J. Comput. Chem.* **1990**, *11*, 361.

(32) Carey, F.; Sundberg, R. *Advanced Organic Chemistry*, 3rd ed.; Plenum Press: New York, 1990; Part A, p 221.

(33) (a) Takezaki, M.; Hirota, N.; Terazima, M.; Sato, H.; Nakajima, T.; Kato, S. *J. Phys. Chem. A* **1997**, *101*, 5190. (b) Rubio-Pons, O.; Loboda, O.; Minaev, B.; Schimmelpfennig, B.; Vahtras, O.; Agren, H. *Mol. Phys.* **2003**, *101*, 2103.

(34) The Gibbs free energies are considered; however, for simplicity and fluency when reading text the energy expression is used instead of Gibbs free energy.

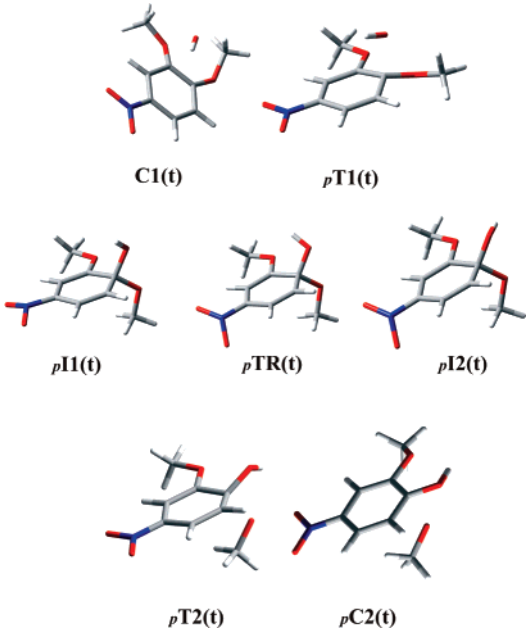

FIGURE 1. Molecular models of important geometries involved in the reactions: initial complex **C1**, transition state for the addition step **T1**, first intermediate **I1**, rotational transition state between intermediates **TR**, transition state for the elimination step **T1**, final complex **C2**. In this work, the prefix ***m***- or ***p***- indicates that the given structure corresponds to the meta or the para reaction, respectively. Structures without a prefix (**C1(s)**, **C1(t)**) belong to both reaction paths of a given multiplicity. Symbols in parentheses (**(s)** or **(t)**) are indicative of the electronic state involved (S_0 or T_1).

corresponding to the addition step is higher for para and lower for meta substitution in the triplet state. In contrast, the para attack is more favorable than the meta attack in the singlet ground state.

The elimination step in the meta reaction path is predicted to have the highest energy barrier in the triplet state (Table 1). However, experimental and mechanistic studies show that the meta product is formed exclusively and in less than 0.5 μs. In addition, the intermediates corresponding to the other pathways (para, ortho, and ipso) are detectable after this period.[6] These facts lead us to assume that the reaction is a diabatic process (for the classification of photoreactions suggested by Turro, see Figure 3[35]) and a radiatonless jump takes place from the excited surface to the singlet manifold along the reaction path, before the elimination, in the intermediate region. Using CAS-SCF calculations Takezaki et al. have shown that the T_1/S_0 intersystem crossing of nitrobenzene is controlled by the fluctuation of the nitro group along its bending mode.[33a] Accordingly we investigated the curvature of the lowest triplet and singlet potential surfaces, along the out-of-plane bending motion of this group, for the geometry in the first para and meta intermediates (***p*I1[NV](t), *m*I1[NV](t)**). The main difference between the meta and para σ-complex geometries in the triplet state lies in the arrangement of the nitro group around the unsaturated ring. It is predicted to be planar for meta while strongly bent (bending angle[36] $\delta \approx 20°$) for para intermediates (Scheme 4). Furthermore, the C−N bond is significantly shorter while the N−O bonds are somewhat shorter in ***m*I1(t)** than in ***p*I1(t)**.

(35) Reference 2, p 73.

(36) The angle δ is defined as the angle between the plane of the benzene ring and the plane of the O−N−O triangle (see also Scheme 4).

The energies calculated at nine bending angles of the NO_2 group for meta and para intermediates are depicted in Figure 4. The vertical S_0-T_1 gaps at the optimized triplet state geometries are 8.44 and 34.14 kcal/mol for meta and para intermediates, respectively. In both cases the matching of surfaces is evident along the out-of-plane bending mode of the nitro group. Although T_1 and S_0 PESs cross each other, direct radiationless transition at the crossing points F_1, F_2, F_3, and F_4 lying approximately 11 and 15 kcal/mol (meta and para) higher than the corresponding minimum of the curve is quite improbable. Since the rate of radiatonless transition depends exponentially on the T_1-S_0 gap (ΔE_{TS})[2,3] in the case of surface matching, the intersystem crossing will probably occur much faster at the geometry of meta intermediates than that of para intermediates. These findings support the time-resolved spectroscopy data that the lifetime of the meta σ-complex is shorter than that of the other intermediates.[6]

(b) Photohydrolysis of Nitroanisoles. Analogously to **NV**, the meta and para pathways of hydrolysis reactions of *o*-, *m*-, and *p*-nitroanisoles were investigated in the triplet state. Our goal was to determine the orientation effect of the methoxy group at different positions. It is generally believed that the methoxy substituent orients the incoming nucleophile to ortho and para positions in excited states.

The photohydrolysis of nitroanisoles occurs via the stepwise reaction profile discussed in detail in the case of **NV**, except for the para substitution of ***o*NA**. In the latter case the rotational transition state and the second intermediate are missing along the pathway. The formation of the only intermediate is followed by the direct elimination of the leaving group. We found that the meta orientation effect of the nitro group is still dominant and the energy barrier corresponding to the first transition state is always lower for the meta than the para reaction.

If we suppose that the first step is the orientation-determining step, our results suggest that the meta product forms preferentially. It does not meet the experimental observation for ***p*NA**. A good leaving group is required for the product formation from the intermediate. Methoxy is known as a good leaving group in nucleophilic substitutions, and one can conclude the same tendency for the triplet state reaction from Table 1. Namely, depending on the barrier height of the elimination step the substitution completes and the addition step determines the outcome of the reaction. However, if the barrier corresponding to the elimination is too high, the decay of the σ-complex intermediate will lead to the starting material instead of the required product. A representative example is the ***p*NA**, where the rates of formation of the meta intermediates after the addition are much higher than that of the para intermediates, but one could expect that the elimination of the hydrogen anion or radical hardly occurs from meta-σ-complex, while the para-substituted product is easily formed from the para-σ-complex intermediate due to the elimination of the methoxy group. In agreement with this assumption, the maximum quantum yield of the hydrolysis of *p*-nitroanisole was measured about three times as low as that of the *m*-nitroanisole.[7]

However, the crucial role of the methoxy group in the directing effect can be concluded from the barriers corresponding to the first step. Our results support the previous assumptions that electron-releasing substituents, especially the methoxy, have an activating effect and an ortho/para orienting effect in the excited state. For instance, with a methoxy group at the ortho position with respect to the site of attack (**NV(t)**) we observed

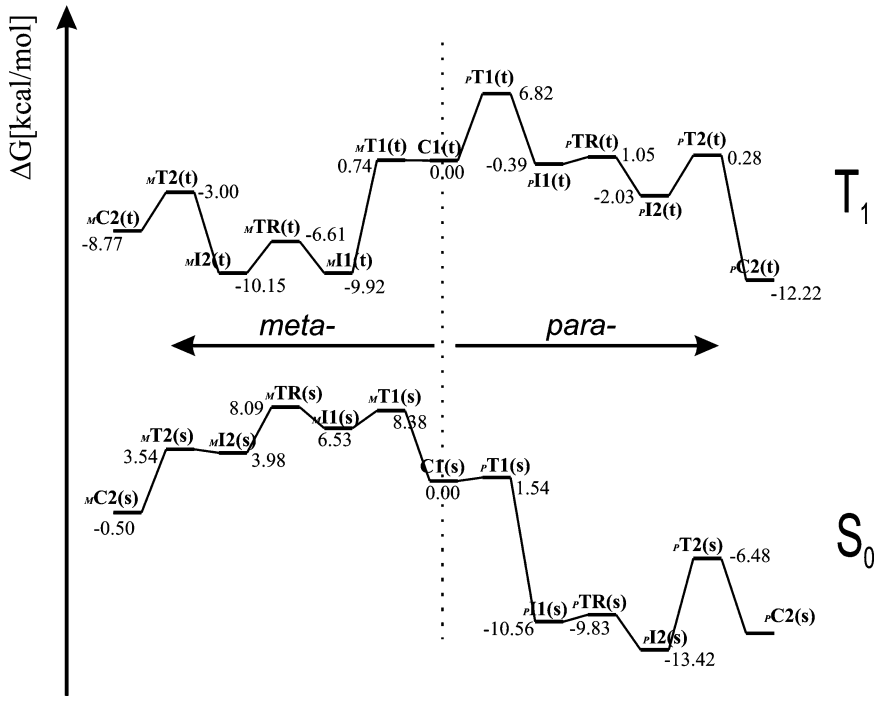

FIGURE 2. The Gibbs free energy profile of the hydrolysis of nitroveratrole in the singlet ground (S_0) and in the triplet ground (T_1) state. The meta (left) and the para (right) pathways start from the same initial complex (**C1(s)**, **C1(t)**).

a lower barrier (6.82 kcal/mol[37]) than without this group (***p*NA**, 8.38 kcal/mol).

We have also thoroughly investigated the effect of the nitro and methoxy group on the π-electron distribution of the benzene ring in both singlet and triplet states (Table 2). In the case of singlet nitrobenzene (**NB(s)**) the NO_2 substituent causes the highest π-electron depletion in ortho and para positions and less in the meta position. In contrast, the density of the π electrons in the triplet state is lower on the meta carbon than on the ortho or para carbons. This result suggests that the nucleophile will attach to the ortho/para carbon in the singlet and to the meta in the triplet state, in agreement with the earlier statement.[2] The methoxy substituent has a strong π-electron-releasing effect and results in a π-electron surplus in the ortho and para positions in both electronic states, so no conclusive statements can be made on these findings.

(c) Photohydrolysis of Chlorinated Nitroanisoles. In the previous part we showed that the leaving group has a large effect on the outcome and quantum yield of the reaction. Next, we want to investigate the effect of halogen substituents, which are known to be good leaving groups in the thermal nucleophilic aromatic substitutions, on the barriers in different steps of the analogous photoreaction. Interchanging a methoxy group of nitroveratrole with chlorine, we obtain 2-chloro-5-nitroanisole (***p*Cl-*m*NA**) and 2-chloro-4-nitroanisole (***m*Cl-*p*NA**) which easily undergo photoinduced nucleophilic aromatic substitution. The photohydrolysis of ***m*Cl-*p*NA** mainly yields 2-methoxy-5-nitrophenol[38] while that of ***p*Cl-*m*NA** gives 2-chloro-5-nitrophenol exclusively,[39] i.e., the substitution occurs at the meta position in both cases.

We observe, similarly to the reaction of nitroveratrole, that the substitution of the methoxy group with OH in the triplet state can be described with a reaction path containing three steps. In contrast, the photochemical substitution of chlorine happens in one step, i.e., its substitution is a concerted reaction. Likewise a switch from a multistep to a single-step mechanism was observed in the ground state aromatic nucleophilic substitution of halobenzenes and halonitrobenzenes with halide anions by Glukhovtsev, Bach, and Laiter.[40] They concluded that the weaker the C−X bond, the lower tendency of the σ-complexes to be a minimum. This is probably also due to the relatively good leaving group property of Cl^- (i.e., its nucleofugality[41]).

The energy barriers for the first step (which is the only step for chlorine replacement) are calculated to be lower for the meta than the para reaction of 2-chloro-5-nitroanisole as well as 2-chloro-4-nitroanisole in perfect accordance with the experimental findings.[37]

Experimentally, it was found that neither the photohydrolysis of *m*-bromonitrobenzene nor that of *o*-bromoanisole[7] yields the meta with respect to the nitro group substituted product. So, when Cornelisse and Havinga investigated the substitution of the meta halogen in 2-chloro-4-nitroanisole and 2-bromo-4-nitroanisole by OH^-, they concluded that "the reactivity of 2-bromo-4-nitroanisole results from combination of *meta*-activation by the nitro group and *ortho*- activation by the methoxy group",[7] since their experiments clearly demonstrate that both substituents are needed to start the reaction. Our calculations indicate that the replacement of chlorine by OH− at the meta position requires the highest amount of energy

(37) The Gibbs free energies were considered.

(38) Sargi Bonilha, J. B.; Tedesco, A. C.; Nogueira, L. C.; Ribeiro Silva Diamantino, M. T.; Carreiro, J. C. *Tetrahedron* **1993**, *49*, 3053.

(39) Nijhoff, D. F.; Havinga, E. *Tetrahedron Lett.* **1965**, 4199.

(40) Glukhovtsev, M. N.; Bach, R. D.; Laiter, S. *J. Org. Chem.* **1997**, *62*, 4036.

(41) (a) Stirling, C. J. M. *Acc. Chem. Res.* **1979**, *12*, 198. (b) Ayers, P. W.; Anderson, J. S. M.; Rodriguez, J. I.; Jawed, Z. *Phys. Chem. Chem. Phys.* **2005**, *7*, 1918.

TABLE 1. Relative Energies and Gibbs Free Energies (in kcal/mol) of the Stationary Points Involved the Thermal and Photonucleophilic Aromatic Substitutions (See Scheme 1 and Figure 1 for numbering)

		UB3LYP/6-311+g(d)				UMP2/6-31+g(d)	
		ΔE		ΔG		ΔE	
		meta	para	meta	para	meta	para
NV(s)	R	34.70	34.70	21.07	21.07	46.99	46.99
	C1	0.00	0.00	0.00	0.00	0.00	0.00
	T1	6.63	0.38	8.38	1.54	3.19	0.99
	I1	5.14	−13.62	6.53	−10.56	0.86	−14.05
	TR	6.88	−12.77	8.09	−9.83	1.90	−13.35
	I2	2.73	−16.43	3.98	−13.42	−1.90	−17.41
	T2	2.91	−7.32	3.54	−6.48	−2.67	−4.73
	C2	−43.48	*a*	−0.50	*a*	−41.22	−45.18
	P	24.56	11.66	17.58	5.68	31.49	25.51
NV(t)	R	60.95	60.95	45.14	45.14	46.99	46.99
	C1	0.00	0.00	0.00	0.00	0.00	0.00
	T1	0.01	6.32	0.74	6.82	10.46	5.49
	I1	−10.79	−0.37	−9.92	0.39	−18.68	−11.47
	TR	−7.84	0.35	−6.61	1.05	−15.83	−10.75
	I2	−11.82	−3.35	−10.15	−2.30	−20.14	−14.98
	T2	−3.00	0.51	−3.00	0.28	6.41	0.21
	C2	−6.68	−11.37	−8.77	−12.22	−3.90	−4.06
	P	50.29	43.91	35.38	29.81	61.99	61.50
oNA	R	53.44	53.44	39.09	39.09	50.84	50.84
	C1	0.00	0.00	0.00	0.00	0.00	0.00
	T1	0.15	6.30	0.97	7.35	9.42	12.09
	I1	−9.46	−5.09	−7.31	−2.70	−14.26	−15.16
	TR	−4.36	*b*	−2.70	*b*	−8.02	*b*
	I2	−4.44		−2.97		−14.26	
	T2	18.87	24.00	17.27	22.44	16.38	21.88
	C2	16.57	19.67	12.42	15.75	3.82	−16.72
	P	91.10	89.86	81.95	81.10	114.26	111.87
pNA	R	60.58	60.58	44.63	44.63	47.51	47.51
	C1	0.00	0.00	0.00	0.00	0.00	0.00
	T1	0.14	8.52	0.93	8.38	6.61	9.25
	I1	−8.89	0.58	−6.89	1.06	−18.79	−14.60
	TR	−4.16	1.62	−2.53	2.03	−13.26	−13.26
	I2	−8.89	0.38	−6.89	0.89	−18.79	−14.96
	T2	22.38	4.59	19.95	3.02	16.46	1.96
	C2	19.76	*a*	15.31	*a*	3.51	−5.42
	P	100.06	48.32	89.62	33.98	127.17	47.97
mNA	R	60.97	60.69	46.00	46.00	59.18	59.18
	C1	0.00	0.00	0.00	0.00	0.00	0.00
	T1	0.94	4.88	2.47	6.61	10.29	8.04
	I1	−10.48	1.20	−8.17	3.81	−18.57	−6.46
	TR	−7.44	4.16	−5.25	6.11	−14.85	−4.28
	I2	−10.48	3.05	−8.17	5.23	−18.57	−4.43
	T2	−2.83	21.79	−2.03	20.98	5.27	19.59
	C2	−8.93	16.82	−9.20	14.48	−3.15	6.31
	P	48.85	95.26	35.41	86.42	59.59	114.24
pCl-mNA	R	64.21	64.21	48.48	48.48	52.86	52.86
	C1	0.00	0.00	0.00	0.00	0.00	0.00
	T1	7.09	0.08	0.99	7.74	9.36	6.33
	I1	−12.87	*c*	−11.44	*c*	−20.70	*c*
	TR	−10.29	*c*	−8.80	*c*	−20.47	*c*
	I2	−12.87	*c*	−11.45	*c*	−20.53	*c*
	T2	−5.31	*c*	−4.82	*c*	3.06	*c*
	C2	−10.71	−43.30	−12.18	−43.60	−8.30	−50.58
	P	49.78	−10.45	35.60	−16.20	56.42	8.49
mCl-pNA	R	64.90	64.90	49.20	49.20	63.56	63.56
	C1	0.00	0.00	0.00	0.00	0.00	0.00
	T1	5.38	8.22	5.60	8.44	10.01	8.78
	I1	*c*	−1.02	*c*	0.00	*c*	−17.28
	TR	*c*	−0.45	*c*	0.41	*c*	−16.41
	I2	*c*	−3.35	*c*	−2.17	*c*	−19.67
	T2	*c*	2.25	*c*	2.09	*c*	−0.23
	C2	−29.16	−8.73	−27.30	−9.99	−48.10	−7.79
	P	−4.07	49.87	−10.63	35.82	3.67	50.77

[a] ***p*C2[NV](s)** and ***p*C2[*p*NA](t)** could not be optimized at the UB3LYP/6-311+g(d) level. [b] In the case of ***o*NA** the rotational transition state and the second intermediate are missing along the para pathway (see text section 3.b). [c] Substitution of chlorine is a concerted reaction (see text section 3.c).

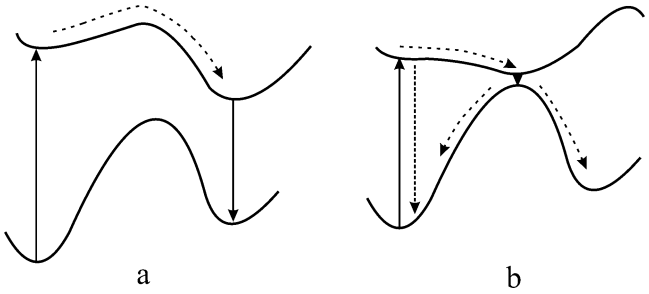

FIGURE 3. Schematic representation of an adiabatic (a) and diabatic (b) photoreaction.[35] The third class of photoreactions, the "hot" ground state reaction, is not shown since it does not play a role in our reaction.

SCHEME 4

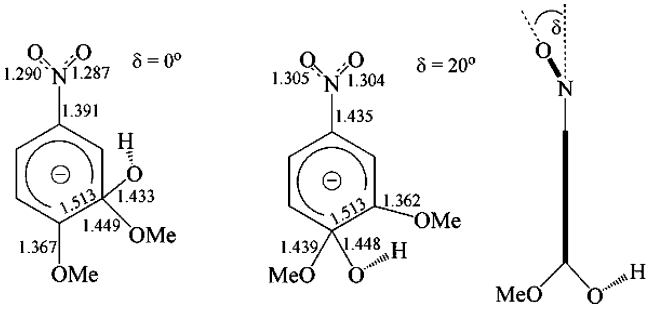

among the meta substitutions in the triplet state considered in this work. In contrast to the previous substituents, bond breaking and bond making was found to occur in a single step.

(d) Solvent Effect. The investigated reactions were performed in the liquid phase; for instance, the photohydrolysis of nitroveratrole was observed occurring in the mixture of water and tetrahydrofuran (98:2). The phase plays a crucial role in the S_N2 reactions: the well-known image of the one barrier reaction profile can be evolved due to the effect of the solvent molecules.[42] In contrast, the gas-phase reaction was found to proceed via a double-well mechanism.[43]

Since σ-intermediates have been detected in the reaction of S_N2 Ar* and S_N2 Ar mechanisms (in the latter the σ-complex is called Meisenheimer complex[44]) the multistep process likely proceeds not only in the gas phase but also in the liquid phase. However, a change in the mechanism when going from the gas into the liquid state still might occur as observed for the S_N2 reactions, since the presence of the solvent molecules may be very important as these reactions involve charged species. To scrutinize the solvent effect on the reaction profile polarizable continuum model (PCM) calculations were carried out for the reference nitroveratrole reaction in triplet state **NV(t)**, using water as solvent. In Table 3 the relative energies and Gibbs free energies (in kcal/mol) are listed for each isomer optimized at the PCM/UB3LYP/6-31+G(d) level.

Similarly to the gas-phase reaction, an addition−elimination mechanism, i.e., the S_N2 Ar*, was observed for the photohydrolysis of nitroveratrole in water. In addition, the same type

(42) (a) Alemán, C.; Maseras, F.; Lledos, A.; Duran, M.; Bertrán, J. *J. Phys . Org. Chem.* **1989**, *2*, 611. (b) Kozaki, T.; Morihashi, K.; Kikuchi, O. *J. Am. Chem. Soc.* **1989**, *111*, 1547. (c) Bickelhaupt, F. M.; Baerends, E. J.; Anibbering, N. M. M. *Chem. Eur. J.* **1996**, *2*, 196.

(43) (a) Olmstead, W. N.; Brauman, J. I. *J. Am. Chem. Soc.* **1977**, *99*, 4219. (b) Pellerite, M. J.; Brauman, J. I. *J. Am. Chem. Soc.* **1980**, *102*, 5993.

(44) Artamkina, G. A.; Egorov, M. P.; Beletskaya, I. P. *Chem. Rev.* **1982**, *82*, 427.

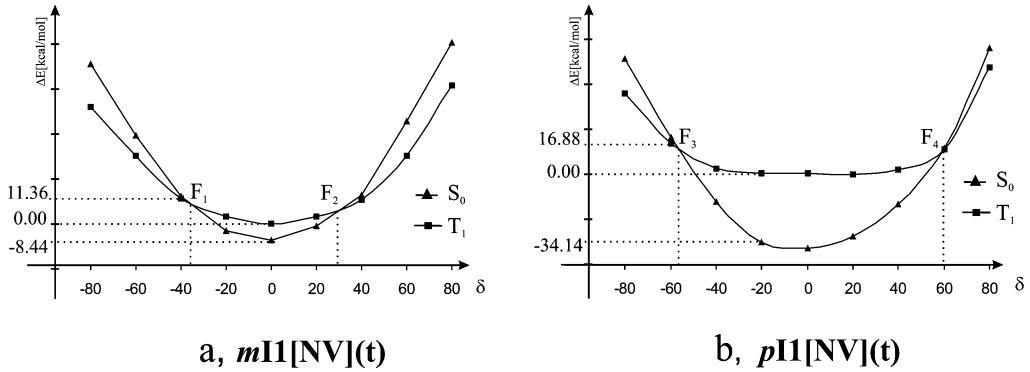

FIGURE 4. Potential curves of the T_1 (■) and S_0 (▲) surface at nine bending angles of the NO_2 group calculated for ***m*I1[NV](t)** (a) and ***p*I1-[NV](t)** (b). All structural parameters except the bending angle (δ) were fixed to the optimum value in the T_1 state.

TABLE 2. Distribution of the π Electrons of Nitrobenzene (NB) and Methoxybenzene (MB) in the Triplet (t) and in the Singlet State (s) at the B3LYP/6-311g(d) Level

	$\sum\pi_{NBO}$		
	ortho	meta	para
NB(s)	0.95	0.99	0.96
NB(t)	1.12	0.93	1.12
MB(s)	1.08	0.99	1.04
MB(t)	1.04	0.98	1.38

TABLE 3. Relative Energies and Gibbs Free Energies (in kcal/mol) of the Stationary Points Involved the Photohydrolysis of Nitroveratrole in the Liquid Phase

		PCM/UB3LYP/6-31+G(d)			
		ΔE		ΔG	
		meta	para	meta	para
NV(t)	R	21.16	21.16	12.45	12.45
	C1	0.00	0.00	0.00	0.00
	T1	0.06	4.08	1.60	6.08
	I1	−19.57	−11.23	−16.07	−7.99
	TR	−17.76	−10.01	−14.39	−6.90
	I2	−20.22	−12.42	−16.32	−8.91
	T2	−5.24	−2.44	−3.51	−0.36
	C2	−10.50	−11.99	−12.08	−12.15
	P	13.29	21.55	2.06	9.67

of stationary points exist along both the meta and para pathways. First a π-complex is formed, then this π-system is broken and the σ-complex intermediates are formed through the transition state of the addition step. In the intermediate region the first σ-complex is converted to the second σ-complex via the rotation of the OH group around the C−O bond, which is followed by the elimination of the leaving group and the formation of the product. As can be seen from Table 3 the stationary points of the meta and para intermediate regions are stabilized by ca. 10 kcal/mol in liquid compared to the gas phase. Moreover, the large endothermicity observed for the gas-phase reactions is decreased by the stabilization of products surrounded by the solvent molecules.

In contrast to the reaction profile, the geometries of ***p*I1[NV]-(t)**, ***p*TS1[NV](t)**, and ***p*I2[NV](t)** differ significantly from that obtained in the gas phase. As was described above, the nitro group is bent about $\delta \approx 20°$ in the gas phase para intermediates. In water, the bent nitro group rotates around the N−C_p (carbon in the para position) axis in ***p*I1[NV](t)**, ***p*TS1[NV](t)**, and ***p*I2-[NV](t)** by 76.9°, 72.6°, and 76.4°, respectively. However, this

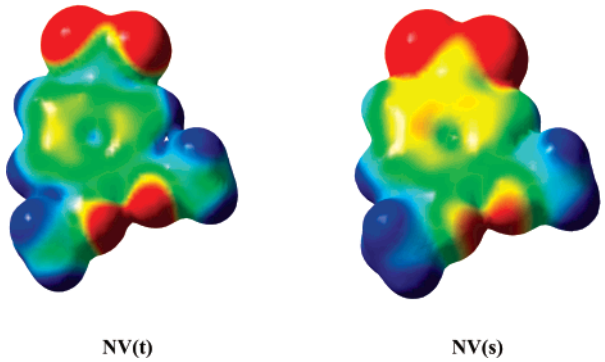

FIGURE 5. Molecular electrostatic potential (MEP) of singlet (a) and triplet (b) nitroveratrole at an isovalue of 0.008. A negative potential is indicated in red; yellow, green, blue, and purple indicate increasingly more positive values of the MEP.

change in geometry is restricted to the intermediate region of the para pathway but it may have a remarkable effect on the whole photoprocess; the necessary condition of the relaxation from triplet states to the ground level is the out-of-plane bending motion of the nitro group. This motion is prohibited by the rotation of NO_2 and this finding thus suggests a longer lifetime for the para intermediates in the triplet state in good agreement with time-resolved spectroscopy measurements.

(e) Prediction of the Regioselectivity. Efficient methods to predict the regioselectivity of nucleophilic photosubstitutions have been in high demand since their discovery. Earlier theories stated that the regioselectivity correlates with charges,[7] HOMO interactions,[13] or the T_1-S_0 gaps at intermediate geometries.[3]

First, we investigated the molecular electrostatic potential (MEP) and we identified those regions in which it is the most positive (Figure 5). These positive regions are the natural destination of an incoming negative charged nucleophile. It must, however, be mentioned that some care should be taken when using this descriptor for nucleophilic attack.[45]

The place of formation (the green areas in the aromatic ring on the electrostatic potential map given in Figure 5) of the

(45) (a) Politzer, P.; Landry, S. J.; Wärnhelm, T. *J. Phys. Chem.* **1982**, *86*, 4767. (b) Sjoberg, P.; Politzer, P. *J. Phys. Chem.* **1990**, *94*, 3959. (c) Tielemans, M.; Promel, R.; Geerlings, P. *Tetrahedron Lett.* **1988**, 1687. (d) Mirejovsky, D.; Drenth, W.; van Duijneveldt, F. B. *J. Org. Chem.* **1978**, *43*, 763. (e) Goldblum, A.; Pullman, B. *Theor. Chim. Acta* **1978**, *47*, 345. (f) De Proft, F.; Amira, S.; Choho, K.; Geerlings, P. *J. Phys. Chem.* **1994**, *98*, 5227.

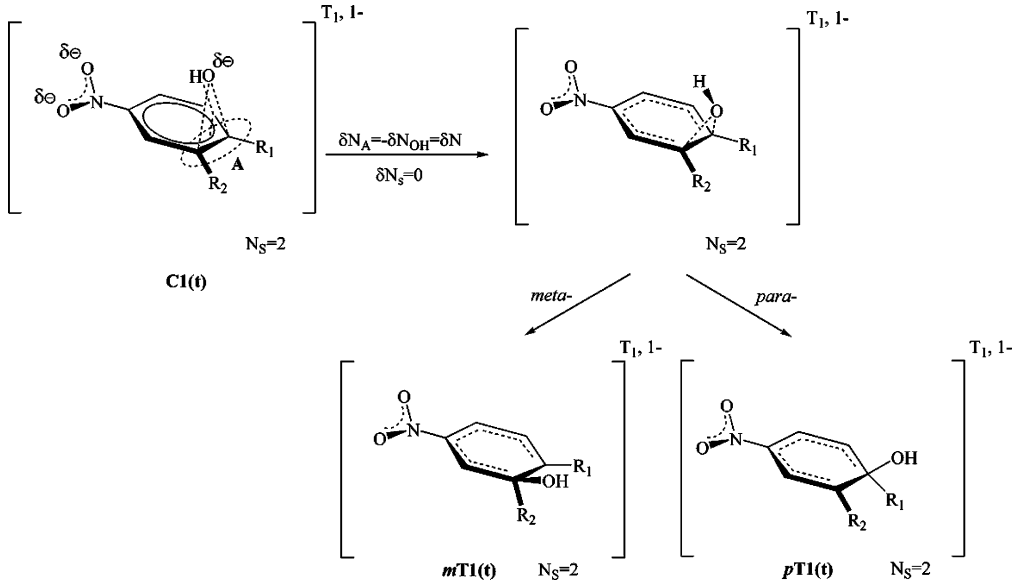

FIGURE 6. Spin-polarized description of the addition step starting from the prereactive π-complex in the photonucleophilic substitutions of aromatic compounds.

prereaction complex, being a charge-controlled process, is clearly predicted by the MEP surface. However, the π-complex has no positional selectivity and different regions above the aromatic ring are activated. The preferred sites in triplet and singlet nitroveratrole, respectively, are above the ipso and para−meta positions and above the para−meta positions. The activated meta and para regions are melting together as is shown in Figure 5. The OH^- is hosted in these regions in the ion−molecule complexes. It is worth mentioning that, in contrast to our above geometry, a planar complex was predicted for halobenzenes.[40] However, we found that a π-complex is more representative to achieve the required attack than a planar complex.

Analyzing the prereaction π-complex we found both partial charge transfer and spin exchange interactions between the arene (A) and the incoming nucleophile (N).[46] Thus, it can be referred electronically as a $^3[^2A^{\delta-} + {}^2N^{\delta-}]$ system, as introduced by Kavarnos and Turro.[47] This finding complicates the regioselectivity prediction of the addition step (the prediction of the primary product) from the reactants. For instance, taking a descriptor for reactants based on charge distribution or frontier molecular orbital method, the prediction of such a descriptor remains valid subject to the formation of the π-complex, in which both the charge distribution and FMO's are changed. As a result, the electrostatic potential and descriptors calculated for the reactants account only for the formation of the ion−molecule complex and not for the regioselectivity in the addition step. The regioselectivity is determined in the σ-complex formation step. This step involves the creation of a bond at a specific position, so one might suggest that the soft−soft interactions are important. Similar considerations, which describe the π-complex formation as a hard−hard interaction and the σ-complex formation as a soft−soft interaction, have been performed for the electrophilic aromatic substitution.[48] Next, we have tried to gain more insight in the prediction of the regioselectivity in the addition step of these photonucleophilic aromatic substitutions. In the π-complexes studied in this work, part of the molecule acts as an electron acceptor (arene) and another part as an electron donor (nucleophile). Thus, considering the attached reactants, the global spin state of the π-complex remains constant during the charge transfer from the donor part to the acceptor part of the molecule. In our case the approaching nucleophile adds to the π system of the aromatic compound to form a σ intermediate. In such a process, the number of electrons is changing from a local point of view (charge transfer occurs from one part of the molecule to another part) at constant global spin number N_S (both the π complex and the σ intermedate are in the triplet state) and the generalized Fukui function $f^+_{NN}(r)$ should be used to investigate the regioselectivity (Figure 6).[49] This index measures the initial response of the electron density to a constrained charge transfer, i.e., the spin number N_S remains constant during the change in the number of electrons. This methodology was recently successfully applied by us in the study of the regioselectivity of radicalar intramolecular cycliza-

TABLE 4. Condensed Spin-Polarized Fukui Functions $f^+_{NN,C}$ Calculated for the Prereactive π-Complexes at B3LYP/6-311g(d) and B3LYP/6-311+g(d) (italic) Levels

	f^+_{NN}			
	meta	para	preferred C in the addition step	experimentally preferred C
C1[NV(t)]	0.16	0.06	meta	meta
	0.15	*0.03*		
C1[oNA]	0.13	0.05	meta	ortho
	0.33	*0.01*		
C1[pNA]	0.15	0.05	meta	para
	0.18	*0.13*		
C1[mNA]	0.10	0.03	meta	meta
	0.40	*−0.26*		
C1[pCl-mNA]	0.11	0.04	meta	meta
	0.10	*−0.11*		
C1[mCl-pNA]	0.12	0.04	meta	meta
	0.06	*0.09*		

(46) Densities and spin densities for **C1NV(t)**: $\rho_S(OH) = 0.592$, $\rho_S(Ar) = 1.408$, $\rho(OH) = 0.274$, $\rho(Ar) = 0.726$.

(47) Kavarnos, G. J.; Turro, N. J. *Chem. Rev.* **1986**, *86*, 401.

(48) Langenaeker, W.; De Proft, F.; Geerlings, P. *J. Phys. Chem.* **1995**, *99*, 6424.

(49) Pintér, B.; De Proft, F.; Van Speybroeck, V.; Hemelsoet, K.; Waroquier, M.; Chamorro, E.; Veszprémi, T.; Geerlings, P. *J. Org. Chem.* **2007**, *72*, 348.

TABLE 5. Charges Based on Electrostatic Potential and Condensed Fukui Functions f_C^+ Calculated for the Reactants at B3LYP/6-311+g(d) and B3LYP/6-311g(d) (italic) Levels

	ChelpG charges		f_C^+			
compd	meta	para	meta	para	preferred C in the addition step	experimentally preferred C
NV(s)	0.27	0.28	0.01	0.07	para	para
	0.24	*0.27*	*0.04*	*0.08*		
NV(t)	0.32	0.23	0.07	0.15	meta	meta
	0.29	*0.22*	*0.07*	*0.07*		
oNA(t)	−0.15	−0.09	−0.09	0.00	meta	ortho
	−0.08	*−0.16*	*0.10*	*0.03*		
pNA(t)	−0.25	0.44	−0.19	0.18	meta	para
	−0.25	*0.42*	*0.06*	*0.08*		
mNA(t)	0.51	−0.31	0.18	−0.11	meta	meta
	0.48	*−0.31*	*0.05*	*0.10*		
pCl-mNA(t)	0.51	−0.12	0.20	−0.15	meta	meta
	0.49	*−0.13*	*0.11*	*−0.02*		
mCl-pNA(t)	−0.06	0.44	−0.40	0.39	meta	meta
	−0.07	*0.43*	*−0.04*	*0.12*		

tions.[49] Moreover, our group has recently been involved in studying other DFT based reactivity indices in these spin-polarized extensions.[50]

So, we have consequently studied the regioselectivity in the different cases considered above using the spin-polarized Fukui function given in (6).

A high value for the $f_{NN,C}^+$ Fukui function is associated with the atom where the density is strongly accumulated upon a nucleophilic attack. On the other hand, low values for these indices correspond to those centers where the electron density changes slightly.

In our cases, the higher local spin-polarized Fukui function value ($f_{NN,C}^+$) at meta or para positions should identify the atom more susceptible to nucleophilic attack. One can indeed observe (Table 4) that $f_{NN,C}^+$ is always higher at the meta position than the para, i.e., showing a preference for the formation of the meta rather than the para intermediate, in good agreement with our earlier findings based on activation barriers. In the cases of ***o*NA** and ***p*NA**, however, experiment shows that the main product of the reaction is not the meta-substituted arene, so the orientation-determining step must be the intersystem crossing or the elimination step. Also, to form the meta product, a fast ISC and a good leaving group are required in the other cases after the formation of the favored meta σ-intermediate.

Table 5 shows the charges and the condensed conventional f_C^+ values (calculated using ChelpG charges) for the meta and para carbons of reactants. However, we found that the charges based on the electrostatic potential reveal the reverse regioselectivity between triplet and singlet nitroveratrole, the population being smaller in the para position for ***o*NA**, ***p*NA**, and ***m*Cl-*p*NA(t)**. Similarly, f_C^+ values show a very poor agreement with experiment; only ***m*NA(t)** and ***p*Cl-*m*NA(t)** have a higher f_C^+ value, i.e., more susceptible to nucleophilic attack, at the meta than the para position. (The prediction for **NV(s)** is in agreement with the experimentally observed outcome.)

In general, it can thus be concluded that the formation of the prereaction complex is a charge-controlled process and is clearly predicted by the molecular electrostatic potential. The σ-complex formation step on the other hand is orbital controlled, as can be clearly seen by the values of the spin-polarized Fukui funtions in Table 4.

4. Conclusion

We have carried out Density Functional Theory (B3LYP) and ab initio (MP2) calculations to explore the reaction mechanism for photonucleophilic aromatic reactions of several nitrobenzene derivatives and to determine the effect of the electron releasing/withdrawing substituents on the reaction profile and on the regioselectivity of the reaction. A multistep reaction profile was found in the triplet state, the replacement of halogen substituents occurring in a single step. We observed that the three processes determining the outcome are the following: (1) the addition step in the excited state, (2) the radiationless transition to the ground state in the intermediate region, and (3) the elimination of the leaving group in the ground state. The solvent effect is taken into account by a continuum model; similarly to the gas-phase reaction a multistep process was found in which the reactants and products are stabilized. The interaction with the solvent causes a significant change in geometry of ***p*I1[NV](t)**, ***p*TS1[NV](t)**, and ***p*I2[NV](t)**.

In a next step, we investigated the regioselectivity using reactivity descriptors emerging from spin-polarized density functional theory. The analysis of the condensed-to-atom spin-polarized Fukui functions on the ring carbon atom $f_{NN,C}^+$ indicates that the correct regioselectivity of the addition step emerges from considering the interaction as a nucleophilic attack on the π-complex species.

Acknowledgment. B.P. thanks the Bizáki Puky Péter Memorial Foundation (Bizáki Puky Péter Emlékalapítvány) and the Hungarian Association of Ph.D. Students (DOSZ) for financial support. T.V. and B.P. thank the Hungarian Scientific Research Foundation (OTKA T048796) for continuous support. F.D.P. and P.G. wish to acknowledge the Fund for Scientific Research-Flanders (Belgium) (FWO) and the Free University of Brussels (VUB) for continuous support of their research group.

Supporting Information Available: Cartesian coordinates of all molecules investigated in this study at the B3LYP/6-311+G(d), MP2/6-31+G(d), and PCM/UB3LYP/6-31+G(d) levels. This material is available free of charge via the Internet at http://pubs.acs.org.

JO701392M

(50) (a) Chamorro, E.; De Proft, F.; Geerlings, P. *J. Chem. Phys.* **2005**, *123*, 084104. (b) Chamorro, E.; De Proft, F.; Geerlings, P. *J. Chem. Phys.* **2005**, *123*, 154104. (c) Chamorro, E.; Perez, P.; De Proft, F.; Geerlings, P. *J. Chem. Phys.* **2006**, *124*, 044105.